

Determination of the Optimal Buoy Shape for A Concept Wave Energy Converter to Harness Low Amplitude Sea Waves using Numerical Simulation

Olakunle Kayode¹, Olufemi Adebola Koya², Titus Oluwasiji Ajewole³

(Received: 30 August 2019 / Revised: 15 September 2019 / Accepted: 29 September 2019)

Abstract— this research investigates the optimal buoy shape for a conceptual point absorber Wave Energy Converter (WEC) for harnessing low amplitude sea waves characteristic of the Gulf of Guinea coast. It has been established that shape of buoy is one of the main parameter affecting the efficiency of a point absorber WEC. Based on best buoy shapes as reported in literature, two shapes are selected for comparison: cone-cylinder composite buoy and Concave wedge shaped buoy. The WEC's buoy and the power take off were mathematically modelled as a mass-spring-damper system. The buoys hydrodynamic coefficients were computed using strip theory, while the simulation in the time domain was executed using MATLAB. Impute parameters referred to as the sea states, in five levels, were described by the significant wave height H_s and the corresponding energy period T_e , typical of the gulf. Output parameters are displacement, velocity, acceleration and force of the buoys, as well as the instantaneous power output of the WEC. For the levels considered, the optimum sea state for the two buoys peaked at level 4 ($H_s = 1.5$ m, $T_e = 14$ s), with concave wedge buoy having an optimal power output of 8 kW while that of cone-cylinder being 3.7 kW. For the other levels the wedge buoy also consistently gives relatively greater power output than the cone cylinder buoy.

Keywords—buoy shape, low amplitude waves, wave amplifying device, wave energy converter.

I. INTRODUCTION

The rising cost of fossil fuels as well as negative impact of such energy sources on global climate is raising opposition to their utilization. As a consequence, in recent years, the demand for renewable energy is increasing and gaining wider acceptance. When compared with various sources of renewable energy such as wind and solar, sea wave energy has higher energy density, is fairly predictable, more reliable and fairly constant on seasonal basis [1]. Globally, the best wave climates, whose annual average power levels are between 20 and 70 kW/m or higher, are found in zones from 30° to 60° latitude [2]. However, attractive wave climates are found also within $\pm 30^\circ$ latitude, where the lower power level (as a result of relatively lower amplitude waves) is compensated by smaller power variability [3]. Nigeria coastal belt is located within the later zone, precisely on the Gulf of Guinea between latitudes 04° 30' and 06° 30'N of the equator. There are many isolated Nigeria coastal communities not connected to the national grid. Diesel generators are a major source of electricity in these isolated coastal communities. Since the power production per unit price of a diesel generator is higher than that of national grid, renewable energy sources in these communities are cost competitive. That most of these communities rely on diesel power generators had been

highlighted by [4][5], thus harnessing the low amplitude wave energy of the region may be a solution to their energy needs. However United Nations Environment Programme report [6] states that studies have shown that West African sub-region has the potential annual wave energy of 300 MWh/m of wave crest which is far below the highest reading of 535 for the north Atlantic ocean (latitude 30° to 60°). Based on this, the report concluded that the future of wave energy in West African is not encouraging, unless a process is developed that can economically utilize relatively the region's small and irregular wave formations.

In recent years, several kinds of ocean power converter prototypes have been developed, according to the expertise of each inventing team and/or specific issues from the local sea where it was planned for. In fact, Wave Energy Converter (WEC) design is still in its infancy with significant research being devoted to quest for more efficient and reliable designs. So far, no typology has provided a clear advantage over others in term of efficiency, cost of production, and maintenance requirements, thus new devices continues to be conceived [7]. There are more than 20 wave energy projects around the world. Nearly all of which are still at pilot stage either as a proof of concept or as part of a research facility. Some are connected to the local grid but none are contributing significantly to a national grid [8][9].

Olakunle Kayode, Department of Mechanical Engineering, Osun State University, PMB 4494, Osogbo, Nigeria. E-mail :-

Olufemi Adebola Koya, Department of Mechanical Engineering, Obafemi Awolowo University, Ile-Ife, Nigeria. E-mail :-

Titus Oluwasiji Ajewole, Department of Electrical and Electronic Engineering, Osun State University, Osogbo, Nigeria. E-mail :-

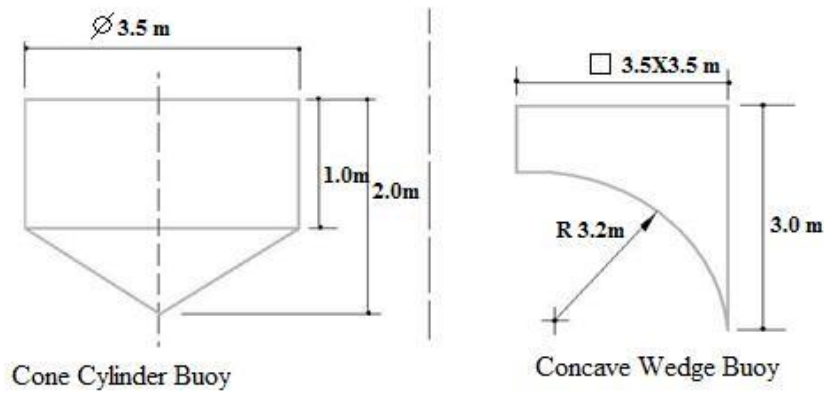


Figure 2. Geometry of the concept WEC buoys

C. Mathematical Modelling of the Concept Device

The WEC's buoy and PTO in the throat section is modelled on the principle of damped forced mechanical vibration, being presented as a mass-spring-damper system as shown in Fig. 3. This approach of modelling point absorber WEC is similar to those employed in [24-

29]. Generally there are six degrees of freedom (Fig. 3, inset) for a floating body, but for the purpose of this study, the primary interface (buoy) is constrained to move only in heave.

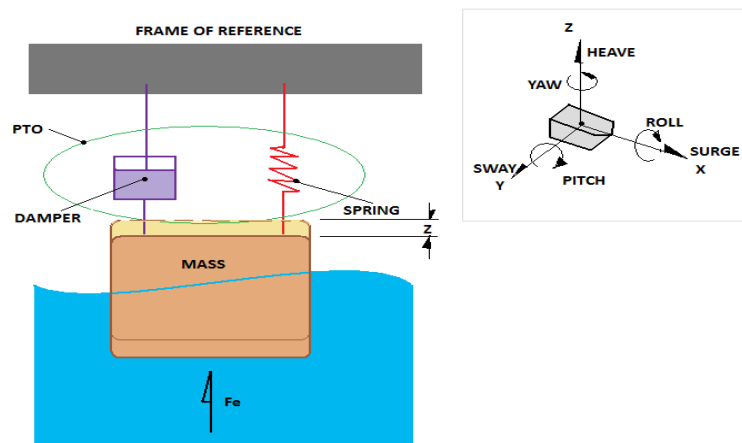


Figure 3. The WEC represented as a mass-spring-damper system.

The PTO model consists of a damper and spring system and the damper was idealized as having viscous (linear) damping. Excitation force of the sea waves was assumed, for simplicity purpose, to be monochromatic. Thus, the equation describing its motion, based on Newton's second law of motion, is given by,

$$M\ddot{Z} = f_h(t) - f_p(t) \quad (2)$$

Where; M is the mass (kg) of the buoy; \ddot{Z} is the buoy's acceleration in heave; f_h is the hydrodynamic force acting on the buoy wetted surface; and f_p is the force exerted by the PTO mechanism. The heave f_h is the sum of three forces, thus:

$$f_h = f_e + f_r - f_{hs} \quad (3)$$

Where f_e is the excitation force from incident wave; f_r is the radiation force due to the buoys motion in water; and f_{hs} is the hydrostatic force. The hydrostatic force is expressed as:

$$f_{hs} = -\rho g S Z \quad (4)$$

Where ρ is the density of the sea water (in kg/m^3); g is the acceleration due to gravity (m/s^2); S is the cross sectional

area of the buoy at the water plane; and Z is buoy's displacement in heave (m).

Thus, equation 2 is expressed as:

$$M\ddot{Z} = f_e + f_r - \rho g S Z + f_p \quad (5)$$

With f_r decomposed to:

$$f_r = -A\ddot{Z} - B\dot{Z} \quad (6)$$

Where A and B are added mass (kg) and radiation damping (kg/s), respectively; and \dot{Z} is buoy's velocity in heave (m/s). The coefficients were computed using the Strip Theory method [30], for given wave natural (angular) frequency and body geometry. f_p is expressed as:

$$f_p = -C\dot{Z} - KZ \quad (7)$$

Where C and K are PTO damping (that is, when acting as a generator) and PTO spring (when acting as a motor), respectively. Since it is desired that the PTO act as generator only, the spring constant in equation 7 is ignored. Therefore, equation 3.3 was re-written as:

$$(M + A)\ddot{Z} + (B + C)\dot{Z} + (\rho g S)Z = f_e \quad (8)$$

For regular waves of (angular) frequency ω_w , the excitation force (f_e) is a simple harmonic function of time (t), expressed as:

$$f_e = F_e \cos(\omega_w t) \quad (9)$$

Where F_e is the amplitude of the excitation force (N) and ω_w is the regular wave frequency (Hz).

The general solution of equation (8) is obtained by adding a particular solution of equation (9) to the complementary solution of the homogeneous equation (i.e. $f_e = 0$ in equation 8). The complementary function represents a transient motion, which is eventually damped out; while the particular solution leads to steady state, which is the focus of this model. The amplitude of the excitation force is obtained as [31]-[32],

$$F_e = \sqrt{\frac{2 \cdot \rho \cdot B \cdot g^3}{\omega_w^3}} \cdot A_w \quad (10)$$

Where, A_w is the incident wave amplitude (m). Hence, equation 8 takes the form of;

$$(M + A)\ddot{Z} + (B + C)\dot{Z} + (\rho g S)Z = \sqrt{\frac{2 \cdot \rho \cdot B \cdot g^3}{\omega_w^3}} \cdot A_w \cos(\omega_w t) \quad (11)$$

According to [31], the optimal conditions for extracting the maximum wave energy are:

- i) The natural oscillation frequency of the oscillating system must equal the wave frequency, that is, a condition of resonance must exist. That is:

$$\omega_{sys} = \omega_w \quad (12)$$

- ii) The damping force coefficient for the PTO must equal the radiation damping coefficient. That is:

$$B = C \quad (13)$$

The hydrodynamic coefficients (added mass and radiation damping) were computed using strip theory. Based on the theory, the buoy was split into a number of transverse panels or strips. Each strip was treated as a two dimensional section in order to compute its hydrodynamic characteristics. Each strip individual coefficient was then integrated along the entire length of the buoy to obtain the buoy's overall coefficients.

D. Simulation of the concept device

Simulation of the WEC system in the time domain was executed using the Matrix Laboratory (MATLAB R2009a). The simulations were used to obtain the buoy's displacement, velocity, and acceleration, while the power extracted by the PTO was obtained using:

$$P = C(\dot{Z})^2 \quad (14)$$

Duration of each simulation was sixty seconds and waves with different amplitudes and periods typical of the Gulf of Guinea coast of Nigeria are employed (as derived from www.buoyweather.com). The impute parameters, constituting the sea states, are described by both the significant wave height H_s and the corresponding energy period T_e . Shown in Table 1 are the sea states used as imputes in the simulations.

TABLE 1.
SEA STATES PARAMETERS USED FOR THE SIMULATION

Sea state	H_s (m)	T_e (s)
1	0.4	08
2	0.8	10
3	1.2	12
4	1.5	14
5	2.0	16

H_s = Significant wave height; T_e = Energy period.

The output parameters obtained from the simulations were buoy's displacements, velocity, acceleration and force, as well as the WEC's instantaneous power output. In order to evaluate the device performance, the Capture Width Ratio (CWR) was calculated for each simulated sea state. This measure of performance is a frequently used performance index of WEC technologies [33].The CWR was computed as,

$$CWR = \frac{P_{abs}}{J \cdot D} \quad (15)$$

Where P_{abs} is mean absorbed power, D is device buoy horizontal extent (m) and J is the wave power per unit of wave front length, as given in Equation 1.

III. RESULT AND DISCUSSION

Motion response (displacement, velocity and acceleration) of the concave wedge buoy is as shown in Figures 4a to 4e. The steady state maximum instantaneous velocity increases from 0.2 m/s for sea state 1 up to 0.47 m/s for sea state 5, and for a fixed value of external damping (PTO), the increase in velocity implies greater power output (Equation 13). The maximum instantaneous acceleration values also increases from 0.17 m/s² for sea state 1 to 0.19 m/s² for sea state 5. The figures show that the buoy achieves steady state motion (displacement) from 2.8 seconds for sea state 1 up to 4.7 seconds for sea state 5.

Figures 5a to 5e present the behaviour of the cone-cylinder buoy, which has motion response pattern that is similar to that of concave wedge buoy, except that there is a general reduction in the output parameters' magnitude. The figures show that the buoy achieves steady state motion (displacement) from 2.4 seconds for sea state 1 up to 4.5 seconds for sea state 5; steady state maximum instantaneous velocity increases from 0.15 m/s for sea state 1 up to 0.32 m/s for sea state 5; and maximum instantaneous acceleration values also increases in values from 0.11 m/s² for sea state 1 to 0.13 m/s² for sea state 5. The initial spike in values, observed especially in velocity and acceleration before steady state was achieved, is due to the effect of the complimentary function or general solution of

Equation 8 when set to zero (that is, no external forcing function). This represents a transient motion which is eventually damped out.

The output parameters, when compared for the buoys, shows that for each sea state simulated, the concave wedge buoy consistently gave greater output values for each of displacement, velocity, and acceleration than cone-cylinder buoy. These have implications for power production. Power production depends on the PTO damping factor as well as the buoy velocity (Equation 13), showing that the concave wedge buoy will output relatively greater power than the cone-cylinder buoy.

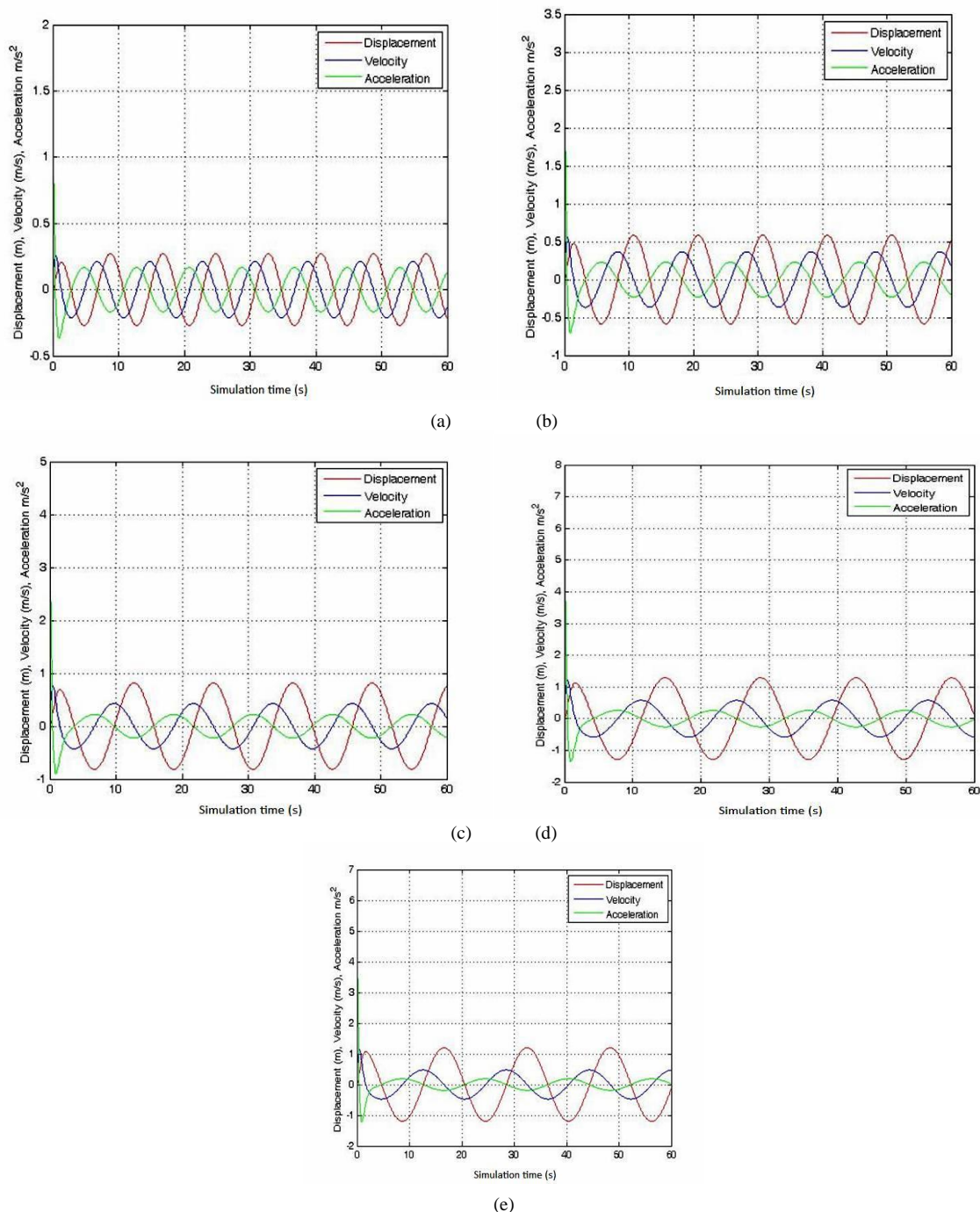


Figure 4. (a) Concave wedge buoy motion response for sea state 1 (Hs= 0.4 m, Te= 8 s), (b) Concave wedge buoy motion response for sea state 2 (Hs= 0.8 m, Te= 10 s), (c) Concave wedge buoy motion response for sea state 3 (Hs= 1.2 m, Te= 12 s), (d) Concave

wedge buoy motion response for sea state 4 ($H_s= 1.5$ m, $T_e= 14$ s), (e) Concave wedge buoy motion response for sea state 5 ($H_s= 2.0$ m, $T_e= 16$ s).

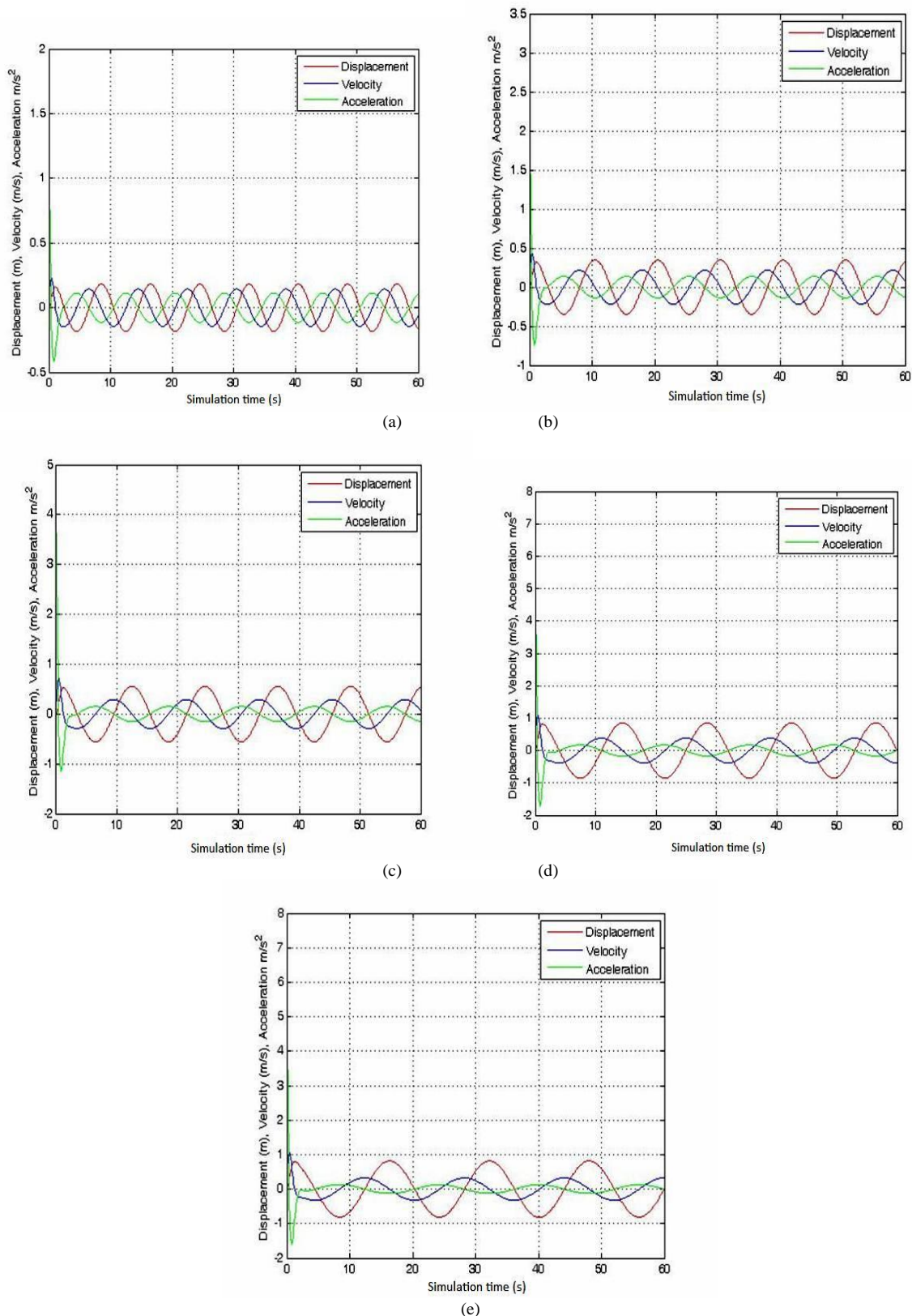


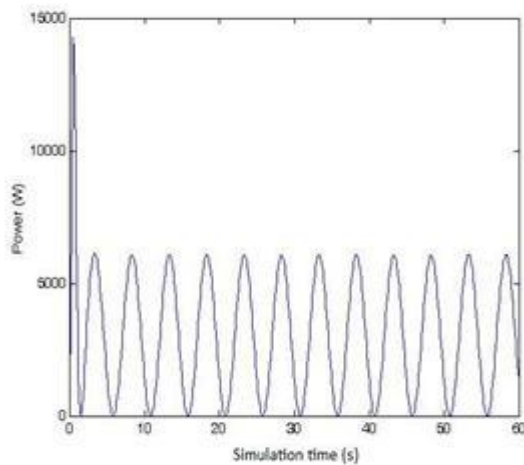
Figure 5. (a) Cone-cylinder buoy motion response for sea state 1 ($H_s= 0.4$ m, $T_e= 8$ s), (b) Cone-cylinder buoy motion response for sea state 2 ($H_s= 0.8$ m, $T_e= 10$ s), (c) Cone-cylinder buoy motion response for sea state 3 ($H_s= 1.2$ m, $T_e= 12$ s), (d) Cone-cylinder buoy motion response for sea state 4 ($H_s= 1.5$ m, $T_e= 14$ s), (e) Cone-cylinder buoy motion response for sea state 5 ($H_s= 2.0$ m, $T_e= 16$ s),

Instantaneous power output of the Concave Wedge buoy is as presented in Figures 6a through 6e, while that of Cone-cylinder buoy is as shown in Figures 7a through 7e. As observed in motion response, the pick

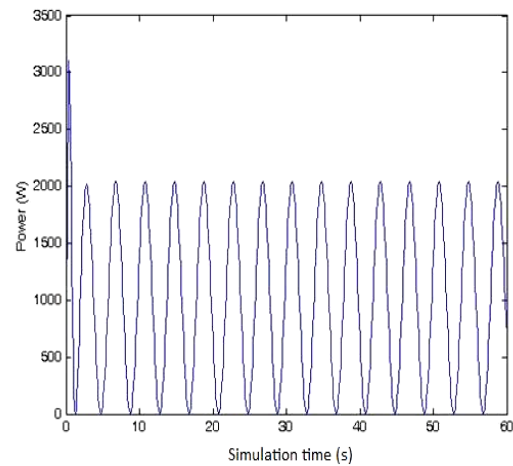
instantaneous power for steady state conditions for the buoys increases with the magnitude of the sea states. For the concave wedge it increases from 2.04 kW for sea state 1 to 10.14 kW for sea state 5, while for

the Cone-cylinder buoy it varies from 0.94 kW for sea state 1 to 4.7 kW for sea state 5. The mean power output for the Concave wedge buoy range from 1.04 kW for sea state 1 to 5.56 kW for sea state 5, with corresponding standard deviations of 0.733kW and 5.96kW respectively. In the case of the Cone-cylinder buoy, the mean power output range from 0.49 kW for sea state 1 to 2.85 kW for sea state 5, with corresponding standard deviations of 0.368 kW and 4.54 kW respectively. The initial high spike in the instantaneous power output for each simulation is due to the effect of transient motion effect on buoy velocity which is eventually damped out as the motion

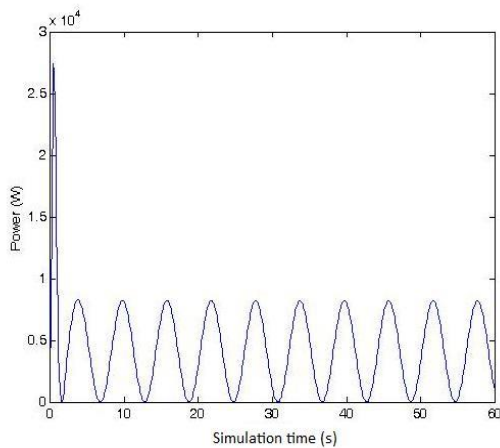
response achieves steady state. The plot of mean output power as against the sea states for the two types of buoys considered is as shown in Fig. 8, while Fig. 9 shows the capture width ratio for the two buoys across the selected sea states. A look at the Fig. 8 shows that the optimum sea state for the two buoys peaked at sea state 4, with concave wedge buoy having an optimal power output of 8 kW and cone-cylinder optimal power output being 3.7 kW. Also deduced from the graphs is that the wedge buoy consistently gives relatively greater power output than the cone cylinder buoy.



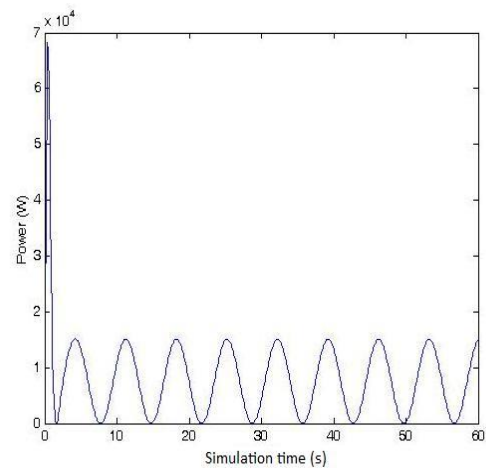
(a)



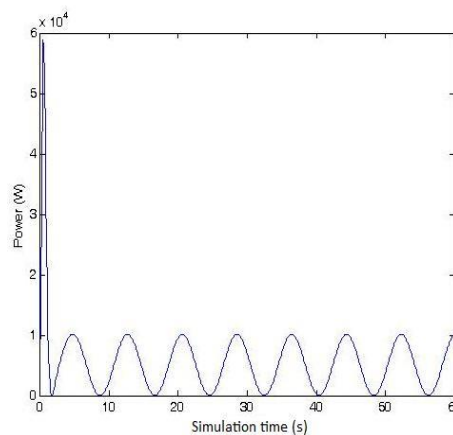
(b)



(c)



(d)



(e)

Figure 6. (a) Concave-wedge buoy instantaneous power output for sea state 1 ($H_s=0.4$ m, $T_e=8$ s), (b) Concave-wedge buoy instantaneous power output for sea state 2 ($H_s=0.8$ m, $T_e=10$ s), (c) Concave-wedge buoy instantaneous power output for sea state 3 ($H_s=1.2$ m, $T_e=12$ s), (d) Concave-wedge buoy instantaneous power output for sea state 4 ($H_s=1.5$ m, $T_e=14$ s), (e) Concave-wedge buoy instantaneous power output for sea state 5 ($H_s=2.0$ m, $T_e=16$ s)

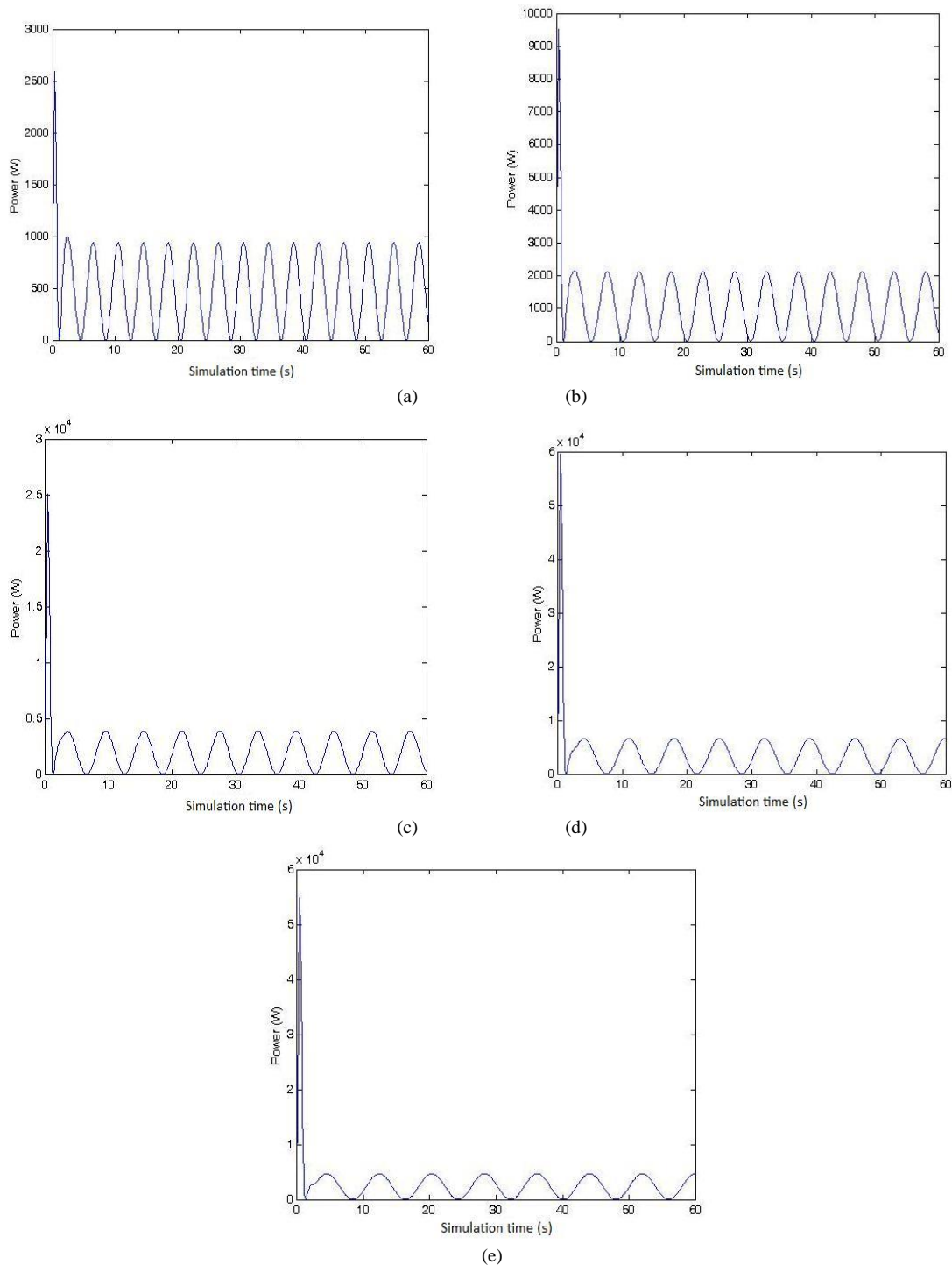


Figure 7. (a) Cone-cylinder buoy instantaneous power output for sea state 1 ($H_s=0.4$ m, $T_e=8$ s), (b) Cone-cylinder buoy instantaneous power output for sea state 2 ($H_s=0.8$ m, $T_e=10$ s), (c) Cone-cylinder buoy instantaneous power output for sea state 3 ($H_s=0.2$ m, $T_e=12$ s), (d) Cone-cylinder buoy instantaneous power output for sea state 4 ($H_s=1.5$ m, $T_e=14$ s), (e) Cone-cylinder buoy instantaneous power output for sea state 5 ($H_s=2.0$ m, $T_e=16$ s)

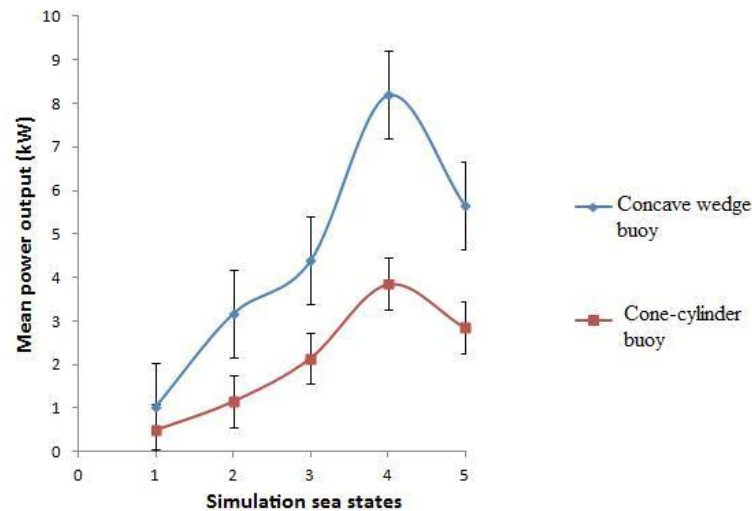


Figure. 8. Mean power output versus Sea state for the concave wedge buoy and cone-cylinder buoy

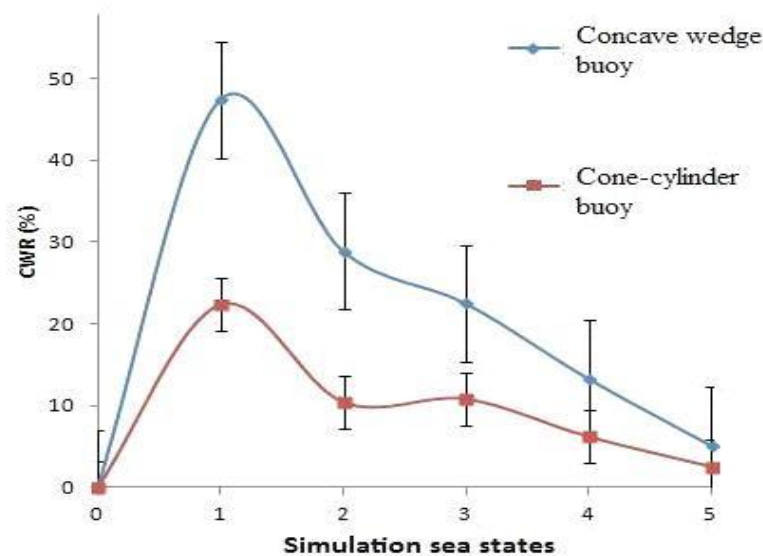


Figure. 9. Capture width ratio of the two buoys investigated as a function of simulation sea states.

IV. CONCLUSION

For the five sea state levels considered, the mean power output for the two buoy is lowest at sea state 1 ($H_s = 0.4$ m, $T_e = 8$ s) at 1.04 kW and 0.49 kW for Concave wedge shaped buoy and cone-cylinder composite buoy respectively. However, the optimum sea state for the two buoys peaked at sea state 4 ($H_s = 1.5$ m, $T_e = 14$ s), with concave wedge buoy having an optimal power output of 8 kW and cone-cylinder optimal power output being 3.7 kW. Also deduced from the graphs is that the wedge buoy consistently gives relatively greater power output than the cone cylinder buoy. The concave wedge buoy is thus the one with optimum power output among the two shapes considered as being appropriate for the concept point absorber WEC. Though the optimal power output is modest, this may be improved upon by mounting several similar buoys in the throat section, and the amplification of the incident wave energy content by the WAD will significantly increase energy output per

buoy, bearing in mind that the wave parameters as presented by nature was used for the simulation.

REFERENCES

- [1] Bosma, B. 'On the Design, Modelling, and Testing of Ocean Wave Energy Converters. Ph.D. dissertation submitted to School of Electrical Engineering and Computer Science, Oregon State University, Corvallis, Oregon, USA; 2013.
- [2] Gunn, K., and Stock-Williams, C. 'Quantifying the Global Wave Power Resources'. *Renewable Energy*. 2012; 1-9.
- [3] Pontes, M., and Falcao, A. 'Ocean energies: Resources and utilisation. In *Proceedings of the 18th Congress of the World Energy Council*, Buenos Aires, Argentina. 2001.
- [4] Emmanuel, A. A and Akinbode, T. (2012) 'Communal Facilities in Coastal Settlements of Ondo State, Nigeria: Assessment of Community-Based Organisations' Efforts Using the Facility Contributory Index Model' *British Journal of Education, Society & Behavioural Science* 2(2): 150 - 161.
- [5] Olufayo, O., Omole, F., and Lawanson, T. (2013). 'Utilizing Creeks for Integrated Rural Coastal Development of Ilaje Area of Nigeria'. *Ethiopian Journal of Environmental Studies and Management* 6(3), 294-299
- [6] UNEP. Ocean Energy Potential of the West African Region. *UNEP Regional Seas Reports and Studies*. 1983; no.30.

- [7] Falcao, A.F. 'Wave energy utilization: a review of the technologies' *Renewable Sustainable Energy Rev.* (2010) 14(3): 899-918.
- [8] Akpinar, A. and Kömürçü, M. I. 'Wave energy potential along the south-east coasts of the Black Sea'. *Energy* 42 (2012) 289 – 302.
- [9] Beirao, P. and Malca, C. (2014) 'Design and analysis of buoy geometry for a wave energy converter' *International Journal of Energy and Environmental engineering* (Springer) 5: 91-96
- [10] Pastor, J., and Liu, Y.-C.: 'Hydrokinetic energy overview and energy potential for the Gulf of Mexico'. In: IEEE Green Technologies Conference, Tulsa, OK 2012
- [11] Kim, J. Koh, H.J. Cho, I.H. Kim, M.H., and Kweon, H.M. 'Experimental study of wave energy extraction by a dual-buoy heaving system'. *International Journal of Naval Architecture and Ocean Engineering* 9 (2017) 25-3-4.
- [12] Goggins, J. and Finnegan, W. 'Shape Optimisation of Floating Wave Energy Converters for a Specified Wave Energy Spectrum'. *Renewable Energy* 71 (2014) 208- 220
- [13] Marqués, J., and Torre-Enciso, Y. The Basque Country: A Strategic Commitment to Leading the Wave Energy Sector. *3rd International Conference on Ocean Energy, 6 October, Bilbao, 4 pages.*
- [14] Michailides, C. and Angelides, C. "Modeling of energy extraction and behavior of a Flexible Floating Breakwater," *Applied Ocean Research*, vol. 35, pp. 77–94, 2012.
- [15] He, F., and Huang, Z. "Hydrodynamic performance of pile-supported OWC-type structures as breakwaters: An experimental study," *Ocean Engineering*, vol. 88, (2014). 618–626
- [16] Ning, D., Zhao, X., Goteman, M., and Kang, H. "Hydrodynamic performance of a pile-restrained WEC-type floating breakwater: An experimental study," *Renewable Energy*, vol. 95, (2016) 531–541,
- [17] Zheng, S., and Zhang, Y. "Wave diffraction and radiation by multiple rectangular floaters," *Journal of Hydraulic Research*, vol. 54, no. 1, (2016) 102–115,
- [18] Zhao, X., Ning, D., Zhang, C., Liu, Y., and Kang, H. 'Analytical Study on an Oscillating Buoy Wave Energy Converter Integrated into a Fixed Box-Type Breakwater'. *Mathematical Problems in Engineering Volume 2017*, Article ID 3960401, 9 pages. <https://doi.org/10.1155/2017/3960401>
- [19] Brooks, J. *Elsevier Ocean Engineering Book Series; Wave Energy Conversion*. Elsevier, Amsterdam; 2003.
- [20] Madhi, F., Sinclair, M. E., and Yeung, R. W. The Berkeley Wedge: an Asymmetrical Energy-capturing Floating Breakwater of High Performance. *Marine Systems & Ocean Technology*. (2014); 9 (1): 5-16.
- [21] Hardisty, J. Experiments with Point Absorbers for Wave Energy Conversion. *Journal of Marine Engineering and Technology*. (2012); 11(1): 51-62.
- [22] Sarlak, H., Seif, M. S., and Abbaspour, M. Experimental Investigation of Offshore Wave Buoy Performance. *Journal of Marine Engineering*. (2010); 6(11), 1-11.
- [23] Aderinto, T. and Li, H. Ocean Wave Energy Converters: Status and Challenges. *Energies*. (2018); 11, 1250; 1-26.
- [24] De Backer, G. Hydrodynamic Design Optimization of Wave Energy Converters Consisting of Heaving Point Absorbers. PhD thesis, Faculty of Engineering, Ghent University, Netherlands; 2009.
- [25] Wachter, A. and Nielsen, K. Mathematical and Numerical Modelling of The Aqua BuOY Wave Energy Converter. *Mathematics-In-Industry Case Studies*. (2010); 2: 16-33.
- [26] Engstrom, J. Hydrodynamic Modelling for a Point Absorbing Wave Energy Converter. Ph.D. dissertation, Uppsala University, Sweden; 2011.
- [27] Pastor, J. and Liu, Y. Frequency and Time Domain Modelling and Power Output for a Heaving Point Absorber Wave Energy Converter. *International Journal of Energy, Environment and Engineering*. (2014); 5:101.
- [28] Kim, M. H., and Cho, H. I. A Novel Wave Energy Converter using Relative Motions between Buoy, Submerged Buoy, and Inner Dynamic System. *Proceedings of the 1st Marine Energy Technology Symposium METS13*. April 10-11, 2013, Washington, D.C.
- [29] Lewis, T. M. A Remotely Operated, Autonomous Wave Energy Converter System. Ph.D. Dissertation Department of Electrical and Computer Engineering Oregon State University, Oregon, USA; 2014.
- [30] Journee, J. M. J. Quick strip theory calculations in ship design. *PRADS'92 Conference on Practical Design of Ships and Mobile Structures*, January, 1992, Newcastle upon Tyne, UK.
- [31] Falnes, J. *Ocean Waves and Oscillating Systems*. Cambridge University Press, Cambridge, UK; 2002
- [32] Falcao, A.F. Modelling and controlled of Oscillating body wave energy converters with hydraulic power take off and gas accumulator. *Ocean engineering*. (2007); 34, 2021- 2032.
- [33] Hagerman, G., and Bedard, R. Guidelines for Preliminary Estimation of Power Production by Offshore Wave Energy Conversion Devices, EPRI; 2003
- [34] Waters, R., Rahm, M., Svensson, O., Stromstedt, E., Bostrom, C., Sundberg, J., and Leijon, M. Ocean wave energy absorption in response to wave period and amplitude- offshore experiments on a wave energy converter. *IET Renewable Power Generation*. (2011)5: 465-469.